

Microscopic failure behavior of nanoporous gold

Juergen Biener, Andrea M. Hodge, and Alex V. Hamza

Citation: [Applied Physics Letters](#) **87**, 121908 (2005); doi: 10.1063/1.2051791

View online: <http://dx.doi.org/10.1063/1.2051791>

View Table of Contents: <http://scitation.aip.org/content/aip/journal/apl/87/12?ver=pdfcov>

Published by the [AIP Publishing](#)

Articles you may be interested in

[Alternating brittle and ductile response of coherent twin boundaries in nanotwinned metals](#)

J. Appl. Phys. **116**, 183505 (2014); 10.1063/1.4901472

[Toughness enhancement in hard ceramic thin films by alloy design](#)

APL Mat. **1**, 042104 (2013); 10.1063/1.4822440

[Mechanical properties and scaling laws of nanoporous gold](#)

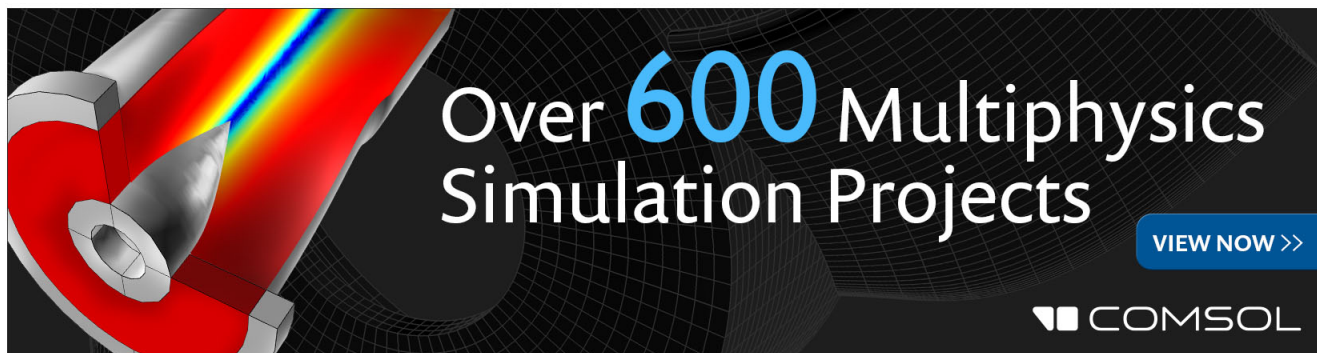
J. Appl. Phys. **113**, 023505 (2013); 10.1063/1.4774246

[Study of hardness and deformation of brittle materials with a density functional theory](#)

J. Appl. Phys. **104**, 053508 (2008); 10.1063/1.2968226

[Nanoporous Au: A high yield strength material](#)

J. Appl. Phys. **97**, 024301 (2005); 10.1063/1.1832742

The advertisement features a dark background with a grid pattern. On the left, there is a 3D simulation of a mechanical part, possibly a turbine blade or a similar component, with a color gradient from red to blue indicating temperature or stress distribution. To the right of the simulation, the text 'Over 600 Multiphysics Simulation Projects' is written in a large, white, sans-serif font. Below this text is a blue button with the text 'VIEW NOW >>' in white. In the bottom right corner, the COMSOL logo is displayed, consisting of a small square icon followed by the word 'COMSOL' in a white, sans-serif font.

Microscopic failure behavior of nanoporous gold

Juergen Biener,^{a)} Andrea M. Hodge, and Alex V. Hamza

Lawrence Livermore National Laboratory, Nanoscale Synthesis and Characterization Laboratory,
Livermore, California 94550

(Received 9 May 2005; accepted 28 July 2005; published online 13 September 2005)

We report on the fracture behavior of nanoporous (np)-Au with an open sponge-like morphology of interconnecting ligaments on the nanometer length scale. Despite its macroscopic brittleness, np-Au is microscopically a very ductile material as ligaments strained by as much as 200% can be observed in the vicinity of crack tips. Cell-size effects on the microscopic failure mechanism were studied by annealing treatments that increased the typical pore size/ligament diameter from ~ 100 nm to ~ 1 μm . Ligaments with diameter of ~ 100 nm fail by plastic flow and necking, whereas failure by slip was observed for larger ligaments with a diameter of ~ 1 μm . The absence of slip marks in 100-nm-sized ligaments suggests a strongly suppressed dislocation activity, consistent with the high yield strength of np-Au. [DOI: 10.1063/1.2051791]

Nanoporous metals have recently attracted considerable interest fueled by potential sensor¹ and actuator applications.^{2,3} One of the key issues in this context is the synthesis of high yield strength materials. Nanoporous Au (np-Au) is a possible candidate due to its monolithic character.² The material can be synthesized by dealloying Ag–Au alloys,⁴ and exhibits an open sponge-like morphology of interconnecting Au ligaments with a typical pore-size distribution on the nanometer length scale.⁵ Previous studies have revealed the brittle nature of np-Au,⁶ and the existence of a ductile-brittle transition as a function of microstructural changes.⁷ In this letter, we go a step further by studying the fracture behavior at both the macro- and microscale, specifically in the context of the brittle-ductile transition previously observed. Key questions in this context are: What causes the macroscopic brittleness of np-Au? Is the normal dislocation-mediated plastic deformation suppressed in nanoscale Au ligaments, or is the brittleness a consequence of the macroscopic morphology? Here, we demonstrate the microscopic ductility of nanometer-sized Au ligaments. The observed fracture behavior seems to be general for nanoporous metals, and can be understood in terms of simple fuse networks.⁸

Recently, we studied the mechanical properties of np-Au (relative density of 0.42) under compressive stress by depth-sensing nanoindentation, and determined a yield strength of 145(± 11) MPa and a Young's modulus of 11.1(± 0.9) GPa.⁹ A striking result of this study is that the experimentally determined value of the yield strength is almost one order of magnitude higher than the value predicted by scaling laws developed for open-cell foams,¹⁰ thus potentially opening the door to the development of a new class of high yield strength/low density materials. This example illustrates that the mechanical properties of nanoporous metals are not yet well understood.

Tensile tests have been performed on (nonporous) nanometer-sized Au contacts.^{11–13} On a microscopic length scale, failure of a single Au ligament in np-Au under tensile stress is closely related to the yielding of nanometer-sized Au contacts which proceeds via quasicontinuous neck elonga-

tion involving a series of order-disorder transitions.^{11–13} The resulting Au nanowires exhibit a yield strength on the order of 4–8 GPa,^{11,13} which is comparable to the ideal shear strength of Au (~ 5 GPa)¹⁴ in the absence of dislocations.¹⁵ However, larger contacts yield in a fracture-like mode in which the neck abruptly contracts in a catastrophic event.^{11,16} The present study addresses the failure mechanism of np-Au by examining fracture surfaces, with particular emphasis on the relationship between microstructure and macroscopic fracture behavior under tensile stress.

Nanoporous Au with a relative density of 0.42 was prepared by selective electrolytic dissolution of Ag from a Ag_{0.58}Au_{0.42} starting alloy. The grain size of the Ag–Au alloy was in the mm range. The details of alloy preparation and the dealloying procedure can be found in Ref. 9. In short, dealloying was performed by applying an electrochemical potential of ~ 1 V versus a saturated calomel electrode, using 75% nitric acid as an electrolyte. The complete removal of Ag was verified by energy dispersive x-ray spectroscopy, and the morphology of the material was studied by scanning electron microscopy (SEM), transmission electron microscopy, and x-ray diffraction.

In the present study, samples of nanoporous Au were manually fractured using a three-point bending configuration. Bending caused transverse fracture triggered by failure on the tension side, indicating that the material is stronger in compression than in tension. As the crack propagates, the region of tensile stress spreads through the whole sample. The specimens showed no macroscopically visible plastic deformation prior to failure, consistent with brittle fracture. SEM was used for further microstructural characterization of the fracture surfaces. On a micrometer length scale [Fig. 1(a)], the fracture surfaces exhibit both apparently featureless regions (I) and regions with a “rock candy” appearance (II). Rock candy features are a characteristic sign of intergranular brittle fracture, where the crack path follows the grain boundaries.¹⁷ However, transmission electron micrographs reveal that the np-Au samples investigated in the present study exhibit a nanocrystalline grain structure.^{9,18} Thus, the intergranular facets in Fig. 1(a) cannot reflect the grain structure of np-Au, but seem to be a remnant of the coarse-grain microstructure of the Ag–Au starting alloy (see subsequent discussion).

^{a)} Author to whom correspondence should be addressed; electronic mail: biener2@llnl.gov

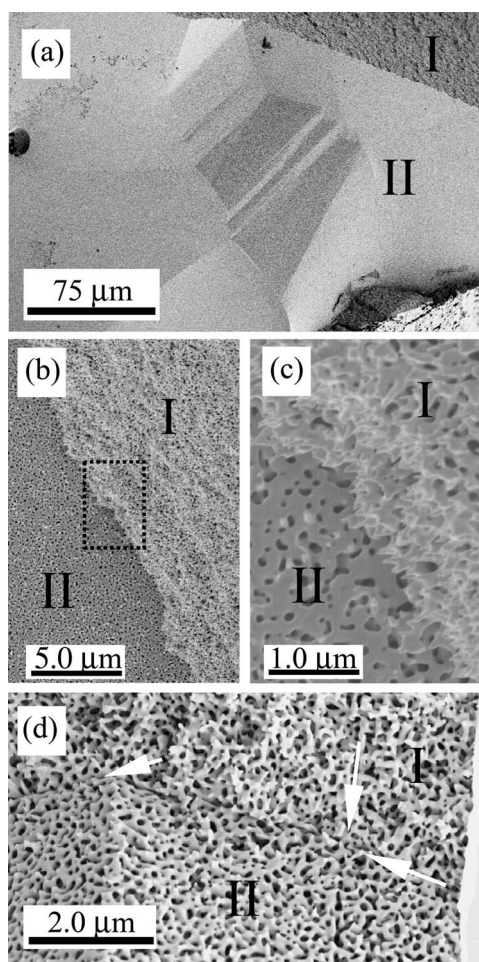


FIG. 1. Microstructure and fracture appearance of nanoporous Au shown at different magnifications. (a) Low-magnification SEM micrograph revealing a combination of transgranular (featureless region I) and intergranular brittle fracture (rock candy region II). (b) Boundary region between transgranular (region I) and intergranular fracture (region II) at higher magnification. (c) A close-up of the outlined area in (b) reveals the ductile nature of the fracture: the ligaments fail by necking due to overloading. (d) Region I (transgranular) and region II (intergranular) are separated by two-dimensional, void-like defects (marked by arrows) that serve as crack nucleation sites.

On a microscopic level, however, characteristic necking features reveal ductile fracture due to overloading of individual ligaments [Figs. 1(b) and 1(c)]. The macroscopically apparently featureless regions (I) of the fracture surface are microscopically very rough and exhibit a high density of disrupted ligaments, whereas the rock candy regions (II) have a very smooth appearance with only a few disrupted ligaments. Extended two-dimensional void-like defects are observed at the boundary between rock candy (II) and featureless (I) fracture surface regions [Fig. 1(d)]. These defects seem to have their origin in a Ag enrichment along the grain boundaries of the original Ag–Au alloy: dealloying of the silver-enriched material leads to the development of a reduced density (voids) along the original grain structure. Indeed, Ag surface segregation during annealing has been reported for the Ag–Au system.¹⁹ Thus rock candy regions of the fracture surface are produced by intergranular fracture (intergranular with respect to the grain structure of the Ag–Au starting alloy), and featureless regions indicate transgranular fracture (through the grains of the Ag–Au starting alloy).

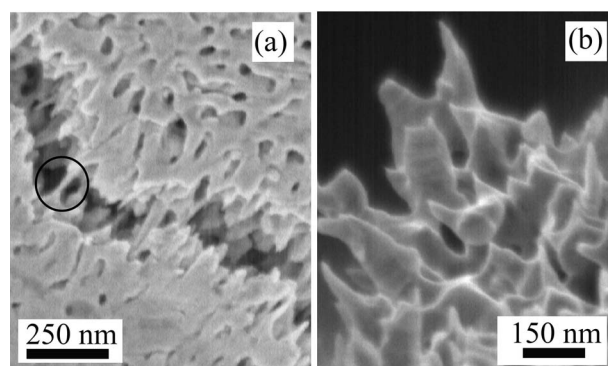


FIG. 2. SEM micrographs showing crack formation during high-load Vickers indents (300 g). (a) High magnification micrograph from a crack tip region showing highly strained ligaments bridging a microcrack. Elongations in the order of 100% have been observed. (b) Detail of a larger crack revealing pronounced necking prior to failure.

The two-dimensional (2D) void-like defects discussed earlier presumably act as crack nucleation sites due to local stress enhancement. Ligaments connecting the regions on opposite sides of a defect experience the highest stress fields and are the first to fail. In case of a penny-shaped defect in a three-dimensional cubic network, the local stress enhancement would be proportional to $n^{1/4}$, where n is the number of missing ligaments.²⁰ Once an unstable crack is formed, the crack propagates along the 2D defects until intersecting with another 2D defect at an oblique angle, where the fracture may or may not switch from “intergranular” to “transgranular.”

The deformation of np-Au in the vicinity of crack tips was further studied by controlled introduction of microcracks via high-load Vickers indents (load of 300 g, maximum indentation depth $\sim 35 \mu\text{m}$). SEM micrographs reveal that microcracks nucleate and propagate along the indenter edges where the stress is concentrated. Individual ligaments, still bridging the crack, can be observed in the vicinity of the crack tips [Fig. 2(a)]. Some of these ligaments are strained by as much as 200%. High magnification micrographs of larger cracks formed in the same area reveal pronounced necking prior to failure [Fig. 2(b)]. The observation of ligaments bridging microcracks suggests that, on a nanometer length scale, the elongation to failure is on the order of 100%, which is a remarkable result in the context of the macroscopic brittleness of np-Au. However, the observed high strain values are consistent with the fact that Au is the most malleable metal, and indeed even higher strain values might have been expected. Nevertheless, microscopically, np-Au is a very ductile material, despite its apparent macroscopic brittleness.

Annealing of np-Au leads to an increase of the length scale of the structure, and thus allows one to study cell-size effects. For example, annealing at 570 °C for a period of 2 h increases the pore size/ligament diameter from $\sim 100 \text{ nm}$ to $\sim 1 \mu\text{m}$. Changes of the fracture mechanism were studied by SEM (Fig. 3). Overall, the fracture morphologies of annealed and unannealed samples are very similar; that is, both featureless (I) and rock candy (II) regions can be observed. However, in the case of the annealed sample, extensive plastic deformation of the nanoporous structure occurs in a larger region around cracks; cell collapse in a layer-by-layer mode indicates regions of compressive stress, and elongation of the cell structure reveals re-

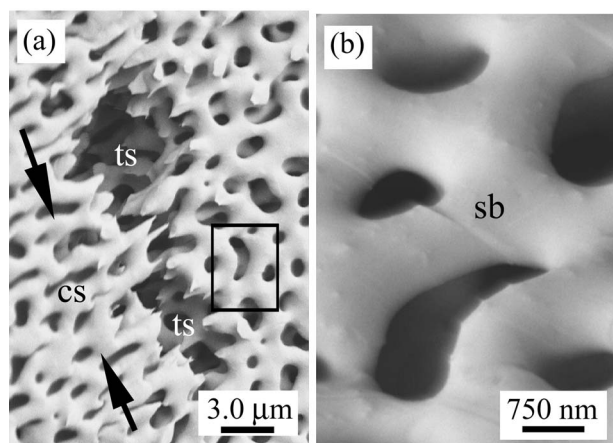


FIG. 3. Fracture surface of a np-Au sample that had been heat treated for 2 h at 570 °C prior to fracture at room temperature. The heat treatment increases the pore size/ligament diameter from ~ 100 nm to ~ 1 μ m. (a) Extensive plastic deformation is observed in a larger region around cracks: cell collapse in regions of compressive stress (cs), and elongation of the cell structure in regions of tensile stress (ts). (b) A higher magnification view of the area within the rectangle reveals plastic deformation of individual ligaments by slip (sb).

regions of tensile stress [Fig. 3(a)]. In addition, plastic deformation of individual ligaments by slip can be detected [Fig. 3(b)]. The slip bands (sb) indicate slip on the $\{111\}$ planes in $\langle 110 \rangle$ direction. It should be emphasized that slip bands were not observed on fracture surfaces of as-prepared np-Au samples [see, e.g., Fig. 2(b)]. Slip plays an important role in the rupture process of thin Au wires; successive slip events on two or more slip systems can lead to necking and failure.²¹ The larger degree of plastic deformation on fracture surfaces of annealed samples indicates strengthening of the network structure. We attribute this to the annealing process, which allows sufficient diffusion (Ostwald ripening) to eliminate the two-dimensional defects that serve as crack nucleation sites. Indeed, SEM reveals that the two-dimensional void-like defects typically observed in as-prepared np-Au samples collapse during annealing, thus fusing weakly connected regions of the network together.

What causes the macroscopic brittleness of np-Au, although it is microscopically a very ductile material? In analogy to the case of a random fuse network analyzed by Kahng *et al.*,⁸ “brittle” failure can be expected for a sufficiently narrow ligament-strength distribution, regardless if the ligaments fail microscopically in a ductile or in a brittle manner. In the limit of a narrow ligament-strength distribution, rupture of the weakest ligament initiates the catastrophic failure of the network structure by overloading adjacent ligaments. The unstable crack then propagates quickly through the bulk of the material following the path of least resistance. This interpretation is consistent with the narrow pore size/ligament width distribution of np-Au, which implies a uniform failure strength.

The overall strength of a randomly fused network is determined by the largest “critical” defect; that is, the defect that causes the highest stress enhancement at its edge.²⁰ In the present study, two-dimensional void-like defects serve as crack nucleation sites by concentrating the stress on adjacent ligaments. Thus, instead of plastic deformation of the whole sample, the failure of a few ligaments triggers the brittle fracture of the network. Interestingly, the failure mechanism

of the ligaments seems to change with the length scale. Microscopic characterization of fracture surfaces of as-prepared np-Au with a ligament diameter of ~ 100 nm suggest that the ligaments fail by plastic flow and necking. On the other hand, failure by slip was observed for ligaments with a diameter of ~ 1000 nm. The latter observation indicates dislocation activity as the stress required to cause slip is reduced by several orders of magnitude by the presence of dislocations.²² The absence of slip marks on fracture surfaces of as-prepared np-Au suggests that the dislocation activity is suppressed by the nanoscale ligament/grain structure. A suppressed dislocation activity at the submicron scale is also consistent with the high strength observed for nanoporous Au,⁹ Au nanocontacts,¹³ and submicron Au pillars.^{23,24}

In conclusion, this study demonstrates that the macroscopic brittleness of np-Au arises from the network structure rather than reflecting a microscopic brittleness. This result may be used to improve the mechanical properties of nanoporous Au; namely, by introducing a broader ligament strength distribution and by eliminating two-dimensional defects.

This work was performed under the auspices of the U.S. DOE by the University of California, LLNL under Contract No. W-7405-Eng-48. The authors would like to thank Professor J. R. Weertman at Northwestern University for helpful discussions, A. Bliss and J. Ferreira at LLNL.

¹K. Bonroy, J.-M. Friedt, F. Frederix, W. Laureyn, S. Langerock, A. Campitelli, M. Sara, G. Borghs, B. Goddeeris, and P. Declerck, *Anal. Chem.* **76**, 4299 (2004).

²J. Weissmueller, R. N. Viswanath, D. Kramer, P. Zimmer, R. Wuerschum, and H. Gleiter, *Science* **300**, 312 (2003).

³D. Kramer, R. N. Viswanath, and J. Weissmueller, *Nano Lett.* **4**, 793 (2004).

⁴R. C. Newman, S. G. Corcoran, J. Erlebacher, M. J. Aziz, and K. Sieradzki, *MRS Bull.* **24**, 24 (1999).

⁵J. Erlebacher, M. J. Aziz, A. Karma, N. Dimitrov, and K. Sieradzki, *Nature (London)* **410**, 450 (2001).

⁶F. Friedersdorf and K. Sieradzki, *Corrosion (Houston)* **52**, 331 (1996).

⁷R. Li and K. Sieradzki, *Phys. Rev. Lett.* **68**, 1168 (1992).

⁸B. Kahng, G. G. Batrouni, S. Redner, L. de Arcangelis, and H. J. Herrmann, *Phys. Rev. B* **37**, 7625 (1988).

⁹J. Biener, A. M. Hodge, A. V. Hamza, L. M. Hsiung, and J. H. Satcher, *J. Appl. Phys.* **97**, 024301 (2005).

¹⁰L. J. Gibson and M. F. Ashby, *Cellular Solids: Structure and Properties*, 2nd. ed. (Cambridge University Press, Cambridge, UK, 1997).

¹¹A. Stalder and U. Duerig, *Appl. Phys. Lett.* **68**, 637 (1996).

¹²U. Landman, W. D. Luedtke, and J. Gao, *Langmuir* **12**, 4514 (1996).

¹³N. Agrait, G. Rubio, and S. Vieira, *Phys. Rev. Lett.* **74**, 3995 (1995).

¹⁴S. G. Corcoran, R. J. Colton, E. T. Lilleodden, and W. W. Gerberich, *Phys. Rev. B* **55**, R16057 (1997).

¹⁵Using the intrinsic yield strength of Au (4–8 GPa) rather than the reported macroscopic yield strength (200 MPa) as an input, the scaling equation predicts a higher yield strength than experimentally observed.

¹⁶A. Stalder and U. Duerig, *J. Vac. Sci. Technol. B* **14**, 1259 (1996).

¹⁷*ASM Handbook* (ASM International, Materials Park, OH, 1992), Vol. 12.

¹⁸A. M. Hodge, J. Biener, L. L. Hsiung, Y. M. Wang, A. V. Hamza, and J. H. Satcher Jr., *J. Mater. Res.* **20**, 554 (2005).

¹⁹K. Meinel, M. Klaua, and H. Bethge, *Phys. Status Solidi A* **106**, 133 (1988).

²⁰P. M. Duxbury, P. L. Leath, and P. D. Beale, *Phys. Rev. B* **36**, 367 (1987).

²¹H. G. F. Wilsdorf, *Acta Metall.* **30**, 1247 (1982).

²²D. Hull and D. J. Bacon, *Introduction to Dislocations*, 4th. ed. (Butterworth-Heinemann, Oxford, 2001).

²³J. R. Greer and W. D. Nix, *Appl. Phys. A: Mater. Sci. Process.* **80**, 1625 (2005).

²⁴J. R. Greer, W. C. Oliver, and W. D. Nix, *Acta Mater.* **53**, 1821 (2005).